OXFORD | **SOT** | **Society of Toxicology**
www.toxsci.oxfordjournals.org

NAD$^+$ Supplementation Attenuates Methylmercury Dopaminergic and Mitochondrial Toxicity in *Caenorhabditis Elegans*

Samuel W. Caito and Michael Aschner[1]

Department of Molecular Pharmacology, Albert Einstein College of Medicine, Bronx, New York 10461

[1]To whom correspondence should be addressed at Department of Molecular Pharmacology, Albert Einstein College of Medicine, 1300 Morris Park Avenue, Forchheimer Rm 2, Bronx, NY 10461. fax: 718-430-8922, E-mail: michael.aschner@einstein.yu.edu.

ABSTRACT

Methylmercury (MeHg) is a neurotoxic contaminant of our fish supply that has been linked to dopaminergic (DAergic) dysfunction that characterizes Parkinson's disease. We have previously shown that MeHg causes both morphological and behavioral changes in the *Caenorhabditis elegans* DAergic neurons that are associated with oxidative stress. We were therefore interested in whether the redox sensitive cofactor nicotinamide adenine dinucleotide (NAD$^+$) may be affected by MeHg and whether supplementation of NAD$^+$ may prevent MeHg-induced toxicities. Worms treated with MeHg showed depletion in cellular NAD$^+$ levels, which was prevented by NAD$^+$ supplementation prior to MeHg treatment. NAD$^+$ supplementation also prevented DAergic neurodegeneration and deficits in DAergic-dependent behavior upon MeHg exposure. In a mutant worm line that cannot synthesize NAD$^+$ from nicotinamide, MeHg lethality and DAergic behavioral deficits were more sensitive to MeHg than wildtype worms, demonstrating the importance of NAD$^+$ in MeHg toxicity. In wildtype worms, NAD$^+$ supplementation provided protection from MeHg-induced oxidative stress and mitochondrial dysfunction. These data show the importance of NAD$^+$ levels in the response to MeHg exposure. NAD$^+$ supplementation may be beneficial for MeHg-induced toxicities and preventing cellular damage involved in Parkinson's disease.

Key words: methylmercury; dopaminergic neurons; mitochondria; *C. elegans*

Methylmercury (MeHg) is a potent neurotoxicant. Studies from mass poisonings in Japan and Iraq, as well as the examination of seafood-rich diets of the Seychelles and Faroe Islands, have illustrated the effects of MeHg on human populations (Ekino *et al.*, 2007; Grandjean *et al.*, 2010). Developmental exposure to MeHg has long-term, latent health effects, including microcephaly and inhibition of neuronal migration, distortion of cortical layers, cerebellar abnormalities, alterations in neurotransmitter systems, and alterations in glial cells (Clarkson and Magos, 2006). In adults exposed to MeHg, damage is more focal, such as loss of cerebellar granular cells and occipital lobe damage (Clarkson and Magos, 2006). Extreme poisonings can lead to ataxia, numbness of extremities, muscle weakness, vision and hearing problems, and paralysis in adults (Clarkson and Magos, 2006). Unfortunately, not much is known about cumulative

exposure over an adult's lifetime and the effects of MeHg on the aging process. It has recently been noted that some of the symptoms associated with MeHg toxicity are similar to those of Parkinson's disease (PD), including loss of motor control and tremor (Landrigan *et al.*, 2005; Petersen *et al.*, 2008; Weiss *et al.*, 2002). PD is the second most common neurodegenerative disease in the United States, and is characterized by the loss of dopaminergic (DAergic) neurons in the substantia nigra pars compacta and locus coeruleus. As less than 10% of PD cases are diagnosed as genetic in origin, environmental factors, such as MeHg, and their contribution to PD etiology have been gaining attention.

Oxidative stress and mitochondrial dysfunction are found in several neurodegenerative diseases, including PD. MeHg generates reactive oxygen species (ROS) H_2O_2, superoxide anion (O_2^-), and nitric oxide (NO) levels in cultured neurons, astrocytes and in rodent brains following MeHg exposure (Farina *et al.*, 2011;

Shanker *et al.*, 2004). Generation of ROS by MeHg may occur either by inhibition of mitochondrial electron transport chain (ETC) complexes II and III, alterations in antioxidant enzyme function, and activation of NO synthase (Herculano *et al.*, 2006; Mori *et al.*, 2007). Additionally, as an electrophile, MeHg reacts readily with thiol and selenol groups on proteins as well with glutathione (GSH), leading to inhibition of enzymes and alteration of protein structure. This has been described for both GSH peroxidase and thioredoxin antioxidant enzymes (Carvalho *et al.*, 2008; Farina *et al.*, 2009). Increased ROS, decreased antioxidant enzyme activity, and depletion of GSH collectively produce an oxidized environment that could affect redox sensitive proteins and cofactors essential for cellular function, such as nicotinamide adenine dinucleotide (NAD^+).

NAD^+ is an essential cofactor required for electron transfer reactions, producing the reduced NADH. NAD^+ is essential for cellular energetics, but also involved in diverse processes as DNA damage repair, cell signaling, and histone deacetylation by acting as a substrate for NAD^+-consuming enzymes (Chini, 2009; Imai and Guarente, 2014; Morales *et al.*, 2014). It is therefore critical that NAD^+ levels be maintained. NAD^+ is synthesized *de novo* from tryptophan in most eukaryotes or can be produced from nicotinic acid or nicotinamide through the action of a salvage pathway (Massudi *et al.*, 2012). Maintenance of NAD^+ levels has been implicated in neurodegeneration associated with Alzheimer's disease and PD. Overexpression of nicotinamide mononucleotide adenylyltransferase 1, an enzyme in the salvage pathway, protects axons from degeneration induced by vincristine or transection in the Wallerian degeneration slow (*wld^s*) mouse and that NAD^+ depletion occurs with axonopathies (Araki *et al.*, 2004; Wang *et al.*, 2005). Prion proteins have been shown to severely deplete intracellular NAD^+ stores, leading to ATP depletion and neuronal death *in vitro* and *in vivo* (Zhou *et al.*, 2015). Similar to prion protein, MeHg has been shown to deplete ATP and NAD^+ levels in mammals (Hamdy and Noyes, 1977); however, the consequences of this depletion have not been investigated. Additionally, NAD^+ supplementation has proven to be neuroprotective. Both intranasal and intracerebral injections of NAD^+ improve motor function in toxic misfolded prion protein-infected mice (Zhou *et al.*, 2015). Exogenous NAD^+ treatment prevents mefloquine-induced neuroaxonal and hair cell degeneration in cochlear organotypic cultures (Ding *et al.*, 2013). NAD^+ supplementation also prevented neuroaxonal degeneration induced by manganese toxicity in cochlear organotypic cultures (Wang *et al.*, 2014). Therefore, we hypothesized that MeHg may alter cellular NAD^+ levels and contribute to DAergic neurodegeneration, and that NAD^+ supplementation may prevent the damage from occurring. We tested this hypothesis by examining DAergic cell morphology and DAergic-dependent behaviors in worms treated with MeHg in the presence or absence of NAD^+ supplementation. Additionally, we examined the effects of NAD^+ supplementation on MeHg-induced oxidative stress and mitochondrial damage that occur simultaneously as the DAergic toxicity.

MATERIALS AND METHODS
Reagents

Unless otherwise stated all reagents were obtained from Sigma-Aldrich (St. Louis, MO).

Caenorhabditis elegans Strains and Handling of the Worms

Caenorhabditis elegans strains were handled and maintained at 20°C on Nematode Growth Medium (NGM) plates seeded with OP-50 strain of *Escherichia coli*, as previously described (Brenner, 1974). The following strains were used in this study: N2, OH7193 (otIs181 [dat-1::mCherry + ttx-3::mCherry]) III; him-8 (e1489) IV), MH1090 (pnc-1(ku212) IV), VP596 (dvIs19[pAF15(gst-4::GFP [green fluorescent protein]::NLS)];vsIs33[dop-3::RFP (red fluorescent protein)], and CB1112 (cat-2(e1112)). All strains were provided by the Caenorhabditis Genetic Center (University of Minnesota), except for the VP596 strain, provided by Dr Keith P. Choe (University of Florida). Synchronous L1 populations were obtained by isolating embryos from gravid worms using a bleaching solution (1% NaOCl and 0.25 M NaOH), and segregating eggs from worm and bacterial debris by flotation on a sucrose gradient, as previously described (Stiernagle, 1999).

MeHg Treatments and Dose-Response Curves

The effect of a 1-h pretreatment of 1 mM NAD^+ on MeHg exposure in *C. elegans* was determined by treating 5000 synchronized L1 N2 worms with doses ranging from 1 to 100 μM for 30 min in 1 ml of M9 liquid buffer at 25°C on an Eppendorf tube rotator. All exposures were carried out in triplicate and repeated four times. After treatment worms were washed three times with M9 buffer, transferred to OP-50-seeded NGM plates, and manually counted for lethality 24 h posttreatment.

NAD^+ Quantification

NAD^+ levels were measured using a commercial NAD^+/NADH quantification kit according to the manufacturer's instructions (BioVision, Mountain View, California). Briefly, treated worms were homogenized in NADH/NAD extraction buffer. Extracts were incubated for 5 min in NAD cycling mix, developer was added, and the absorbency (optical density: 450 nm) was read after 1 h. Data are expressed as ng NAD^+/mg protein.

Dopaminergic Degeneration Assay and Confocal Microscopy

Synchronized L1 OH7193 worms (2500/per tube) were treated with 1 mM NAD^+ ± MeHg (10 or 20 μM). Upon the final wash all worms were plated on OP50-seeded NGM plates. Seventy-two hours posttreatment, 15 worms per condition were mounted onto 4% agar pads (in M9 buffer) and anesthetized with 0.2% tricaine/0.02% tetramisole in M9 buffer. Scoring of neuronal defects was performed using an epifluorescence microscope (Nikon Eclipse 80i) equipped with a Lambda LS Xenon lamp (Sutter Instrument Company) and Nikon Plan Fluor 20× dry and Nikon Plan Apo 60× 1.3 oil objectives, as previously described (Bornhorst *et al.*, 2014). Each worm was blindly scored for the presence of the following morphological changes: puncta formation along dendritic processes, shrunken soma, loss of soma, or loss of dendrites. Representative confocal images of each treatment condition were captured through Plan-Apochromat 20× objective on an LSM510 confocal microscope (Carl Zeiss MicroImaging, Inc) scanning every 200 nm for XZ sections. Images were processed with the Zeiss LSM Image Browser.

Basal Slowing Response

Assessment of DA-dependent behavior was performed using the basal slowing response (BSR) assay, as previously described (Sawin et al., 2000). Briefly, following exposure to NAD^+ and MeHg, L1 worms were seeded on OP-50-spread plates. Three days postexposure worms were washed off the plates with S basal buffer and approximately 10 worms were transferred to either unseeded or OP-50-seeded NGM plates. Locomotor activity was assessed as the number of body-bends per 20 s. Worms deficient in cat-2 (homolog of mammalian tyrosine hydroxylase [TH]) were used as a positive control. Data are presented as the change in body bends, which are calculated by subtracting the number of body bends of worms plated on OP-50-seeded plates from the number of body bends of worms plated on unseeded plates.

MitoTracker Dyes and Fluorescence Quantification

Mitochondrial health was assessed using two MitoTracker dyes (Life Technologies), MitoTracker Green FM to assess mitochondrial mass, and MitoTracker Red CM-H_2XROS to assess mitochondrial membrane potential- and mitochondrial-derived ROS. Twenty thousand L1 worms were incubated with 50 mM Mitotracker dye in the dark for 2 h. Worms were washed three times with M9 buffer and then treated with either NAD^+ or MeHg for 30 min. After three washes, worms were placed on OP-50-spread NGM plates for 2 h, allowing for excess dye to be excreted. OH7193 worms treated with MitoTracker Green FM were loaded onto a 96-well microtiter plate and the green florescence was measured (excitation 485 nm, emission 520 nm). Samples were normalized to worm number by dividing by RFP florescence (read at excitation 544 nm, emission 590 nm). N2 worms treated with MitoTracker Red CM-H_2XROS were loaded onto agar pads and imaged by confocal microscopy. Quantification of red fluorescence was performed using ImageJ 1.36 software as previously described (Gavet and Pines, 2010).

Mitochondrial DNA Copy Number

As a measure of mitochondrial health, relative mitochondrial DNA copy number was measured in worm samples as previously described (Rooney et al., 2015). PCR primers used in determining nuclear DNA content were cox-4 (forward: GC CGACTGGAAGAACTTGTC and reverse: GCGATCACCTTCCA GTA) and nd-1 (forward: AGCGTCATTTATTGGGAAGAC and reverse: AAGCTTGTGCTAATCCCATAAATGT) was used to estimate mitochondrial DNA content.

Oxygen Consumption Rate Analysis

To measure mitochondrial function, oxygen consumption rate (OCR) was measured using the Seahorse XF96 bioanalyzer (Seahorse Bioscience, North Billerica, Massachusetts). Immediately following treatment with 20 μM MeHg in the presence or absence of 1 mM NAD^+ pretreatment, 1000 L1 worms were loaded onto a Seahorse XF96 well cartridge and basal oxygen consumption was measured using a previously described protocol (Luz et al., 2015).

Oxidative Stress Reporter Assay

Activation of SKN-1, the worm homolog of nuclear factor (erythroid-derived-2)-like 2 (Nrf2), was measured using VP596 strain, which expresses GFP under the control of the promoter for the SKN-1 target GSH S transferase 4 (gst-4). These worms also express RFP under the dop-3 promoter. L1 VP596 worms were treated with 1 mM NAD^+ for 1 h ± MeHg (10 or 20 μM) for 30 min. After washing, worms were transferred to a 96-well microtiter plate. Levels of RFP and GFP florescence were measured (RFP: excitation 544 nm, emission 590 nm; and GFP: excitation 485 nm, emission 520 nm). GFP florescence was then divided by RFP florescence to normalize the data to worm number.

Protein Oxidation Quantification

Total protein oxidation was assessed by measuring protein carbonylation using 2,4-dinitrophenylhydrazine (DNPH), as previously described (Yasuda et al., 1999). Briefly, following treatments and wash steps, 50 000 L1 worms were sonicated in 5 mM EDTA with protease inhibitors. Protein was precipitated out of solution by 20% trichloroacetic acid and incubated with 10 mM DNPH for 1 h. Excess DNPH was washed off, samples were suspended in 6 M guanidine hydrochloride, loaded onto a microtiter plate, and absorbance was read at 380 nm. Concentration of oxidized protein was calculated using Beer-Lambert's law and the molar absorptivity coefficient of 21 mM^{-1} cm^{-1} for DNPH. Data were normalized to total protein concentration.

GSH Quantification

Total intracellular GSH levels, ie, reduced and oxidized GSH, were measured using the 5,5′-dithiobis-2-nitrobenzoic acid-GSH disulfide reductase recycling method, as previously described (Caito and Aschner, 2015) in whole worm extracts from 30 000 worms.

Statistics

All statistical analyses were performed using Prism 5 (Graphpad software). Dose-response lethality curves and LD_{50} determination were generated using a sigmoidal dose-response model with a top constraint at 100%. Comparison of LD_{50} values was performed using student's t-test. Statistical analysis of significance was carried out by one-way ANOVA followed by Tukey's post hoc test for all other data. Values of $P < .05$ were considered statistically significant.

RESULTS

NAD^+ Status Affects MeHg Toxicity

As MeHg is a strong electrophile and $NAD+$ is involved in redox status of the cell, we examined whether MeHg affected cellular NAD^+ levels. Total NAD^+ was measured from extracts of N2 worms treated with 10 or 20 μM MeHg for 30 min. Treatment with MeHg caused over a 50% decrease in NAD^+ levels (Figure 1). Worms were then treated with 1 mM NAD^+ for 1 h prior to 30-min treatment with 10 or 20 μM MeHg, doses that are at or below the LD_{50} for MeHg in wildtype (WT) worms. Pretreatment with NAD^+ significantly increased NAD^+ in MeHg-treated worms to the level of untreated control worms (Figure 1).

To assess the effect of NAD^+ status on MeHg toxicity, we exposed WT N2 worms to increasing doses of MeHg in the presence or absence of 1 mM NAD^+ pretreatment for 1 h, and generated dose-response survival curves (Figure 2A). Pretreatment with NAD^+ caused a significant right-hand shift in the dose-response survival curve, increasing the LD_{50} from 20.43 μM for MeHg treatment alone to 34.6 μM. We next examined survival of worms that have diminished cellular NAD^+. Mutant pnc-1

worms, which cannot recycle nicotinamide back into the NAD^+ pool, have over 50% lower NAD^+ levels as compared with N2 (data not shown). Mutant *pnc-1* worms treated with increasing concentrations of MeHg are more sensitive than N2 worms, with an LD_{50} of 3.598 μM as compared with 20.43 μM for N2 (Figure 2B). Pretreatment of *pnc-1* mutants with 1 mM NAD^+ for 1 h prior to MeHg treatment resulted in a dose-response survival curve similar to WT N2 worms. These data suggest that cellular NAD^+ levels are an important determinant of MeHg toxicity.

Increased NAD^+ Levels Attenuate MeHg-Induced DAergic Neurotoxicity

Previously we have shown that MeHg causes DAergic dysfunction in *C. elegans* (Martinez-Finley *et al.*, 2013), therefore we
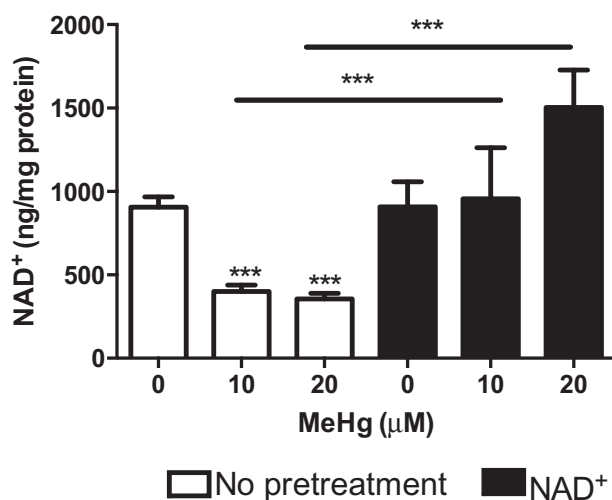

Fig. 1. MeHg decreases cellular NAD^+ levels. N2 worms were treated with 10 or 20 μM MeHg for 30 min. Whole worm extracts were used to measure cellular NAD levels using a spectrophotometric NAD^+ quantification kit. Worms were also pretreated with 1 mM NAD^+ for 1 h prior to MeHg treatment. Data are expressed as mean ng/mg protein ± SEM. All data are representative of four independent experiments. ***$P < .001$ as compared with untreated control. Abbreviations: MeHg, methylmercury; NAD+, nicotinamide adenine dinucleotide.

examined whether increased NAD^+ levels could alter MeHg-induced DAergic neurotoxicity. OH7193 worms, which express mCherry in DAergic neurons, were used to visualize neuronal integrity in worms treated with 10 or 20 μM MeHg in the presence or absence of 1 mM $NAD+$ pretreatment for 1 h (Figure 3). *C. elegans* hermaphrodites have a total of 8 DAergic neurons; 4 cephalic deirids and 2 anterior deirids in the head and 2 posterior deirids in the tail. As previously observed, MeHg significantly alters DAergic cellular morphology 72 h postexposure (Figure 3A). NAD^+ treatment alone looks similar to untreated control worms; however, worms that are pretreated with NAD^+ and then treated with MeHg show significantly healthier looking neurons (Figure 3A). Individual morphological changes were then quantified for the six head DAergic neurons. MeHg dose-dependently increased the number of punctated dendrites in the worms. Although NAD^+ pretreated worms had increased dendritic puncta as compared with untreated worms, there was significantly less damage in the NAD^+ worms treated with MeHg than worms treated with MeHg alone (Figure 3B). MeHg dose-dependently increased the number of shrunken soma in *C. elegans*, which was reduced by NAD^+ pretreatment (Figure 3C). Finally, worms treated with 20 μM MeHg had increased loss of dendrites, which was prevented by NAD^+ pretreatment.

As DAergic neuron morphology was rescued by NAD^+ supplementation, it was next investigated whether DAergic cell functioning was subsequently improved. Previously we have shown that MeHg decreases the BSR in N2 worms; an assay in which N2 worms significantly slow their movement on NGM plates containing a bacterial food source as compared with worms placed on unseeded NGM plates (Sawin *et al.*, 2000). Worms deficient in CAT-2, the nematode homolog of TH, the rate-limiting enzyme for DA biosynthesis, do not show this behavior (Sawin *et al.*, 2000). N2 worms treated with 10 or 20 μM MeHg dose-dependently decrease the BSR similar to the level of *cat-2* deficient worms (Figure 4A). Pretreatment of worms with 1 mM NAD^+ significantly improves the DAergic functioning, similar to untreated control (Figure 4A). Conversely, untreated *pnc-1* mutant worms, which have diminished NAD^+ levels, show significantly lower levels of BSR as compared with untreated control N2 worms (Figure 4B). Mutant *pnc-1* worms show increased susceptibility to MeHg in the BSR
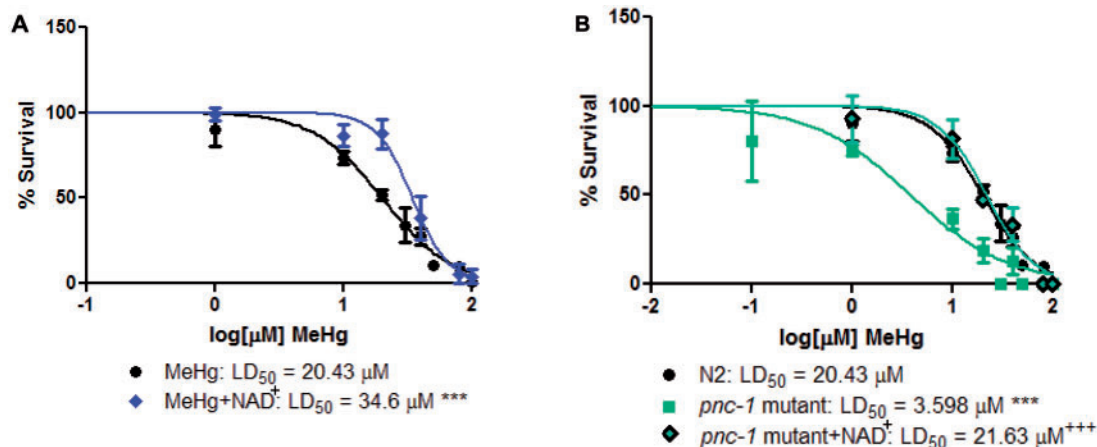

Fig. 2. Altered NAD^+ levels affect MeHg toxicity. A, N2 worms were treated with increasing concentrations of MeHg for 30 min in the presence or absence of a 1 h pretreatment with 1 mM NAD^+. B, *pnc-1* mutant worms were treated with increasing concentrations of MeHg for 30 min in the presence or absence of a 1 h pretreatment with 1 mM NAD^+. Dose-response curves were generated and LD_{50} values were calculated from four independent experiments. ***$P < .001$ as compared with N2 MeHg-treated worms. +++$P < .001$ as compared with *pnc-1* mutant treated with MeHg.

assay, as concentrations of MeHg that do not affect DAergic functioning in N2 (such as 1 μM) cause significantly more loss in the BSR in the *pnc-1* mutants. Altogether the morphologic data and the behavioral data show that physiological NAD$^+$ levels are a requisite for optimal DAeric functioning, and fully reverse the aberrant response to MeHg.

Mitochondrial Health in Response to MeHg Is Improved by NAD$^+$ Supplementation

NAD$^+$ is an important molecule for mitochondrial function, serving roles in oxidative phosphorylation, redox balance, and DNA copy maintenance. Furthermore, mitochondrial function has been implicated in neurodegenerative diseases, such as PD. Therefore, we next investigated measures of mitochondrial health in response to MeHg and NAD$^+$ status. OH7193 worms, which express MCherry in DAergic neurons, were loaded with MitoTracker Green FM and then treated with 10 or 20 μM MeHg in the presence or absence of 1 mM NAD$^+$ pretreatment. Levels of green fluorescence were then measured to determine mitochondrial mass, which was then normalized to worm number dividing by red fluorescence. Twenty μM, but not 10 μM MeHg, decreased mitochondrial mass (Figure 5A). NAD$^+$ pretreatment significantly increased mitochondrial mass in response to 20 μM MeHg (Figure 5A).
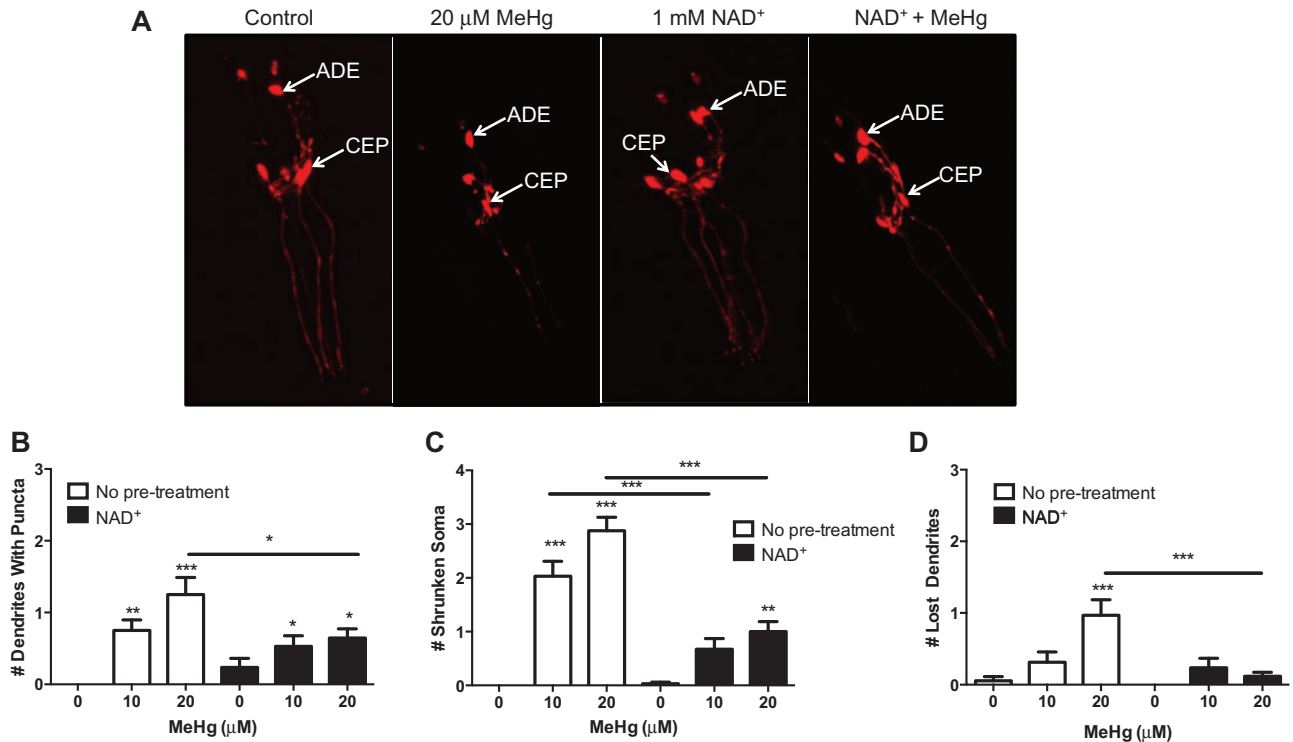

Fig. 3. NAD$^+$ pretreatment attenuates MeHg-induced morphological changes in DAergic neurons. A, CEP and ADE DAergic neurons in OH7193 (dat-1::mCherry) expressing worms were visualized 72 h postexposure to MeHg ± 1 mM NAD+ pretreatment. Arrows indicate the location of the CEP and ADE neurons. Representative confocal images are shown from four experiments. Morphology of the CEP and ADE neurons were examined for 15 worms per treatment group and scored for the number of (B) punctated dendrites, (C) shrunken soma, or (D) lost dendrites. Data are expressed as means ± SEM from four independent experiments. *P < .05, **P < .01, and ***P < .001 as compared with untreated control. Abbreviations: DAergic, dopaminergic; CEP, cephalic deirids; ADE, anterior deirids.
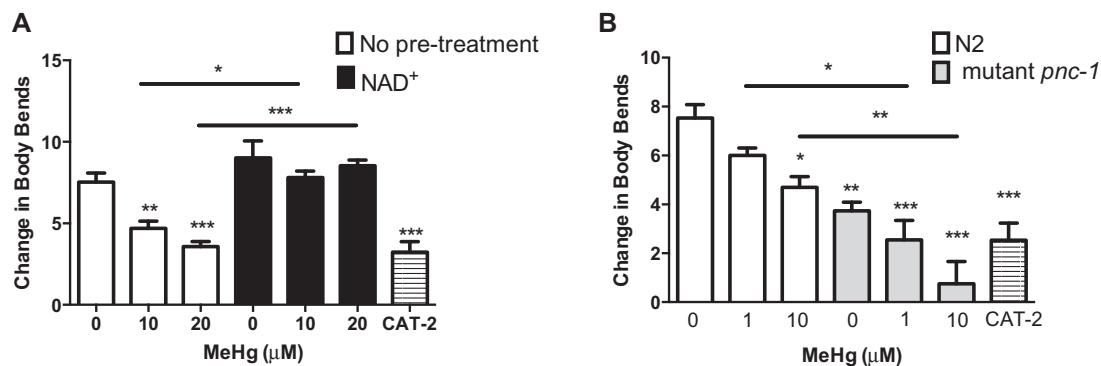

Fig. 4. DAergic-dependent behavior is decreased by MeHg and altered by NAD$^+$ status. A, N2 worms were treated with 10 or 20 μM MeHg for 30 min in the presence or absence of a 1 mM NAD$^+$ pretreatment for 1 h, and DAergic-dependent behavior was analyzed by the basal slowing response assay 72 h posttreatment. B, N2 and mutant pnc-1 worms were treated with 1 or 10 μM MeHg for 30 min and the basal lowing response was analyzed 72 h posttreatment. Worms expressing mutant cat-2 were used as a negative control. Data are expressed as means ± SEM from four independent experiments. *P < .05, **P < .01,***P < .001 as compared with untreated control.
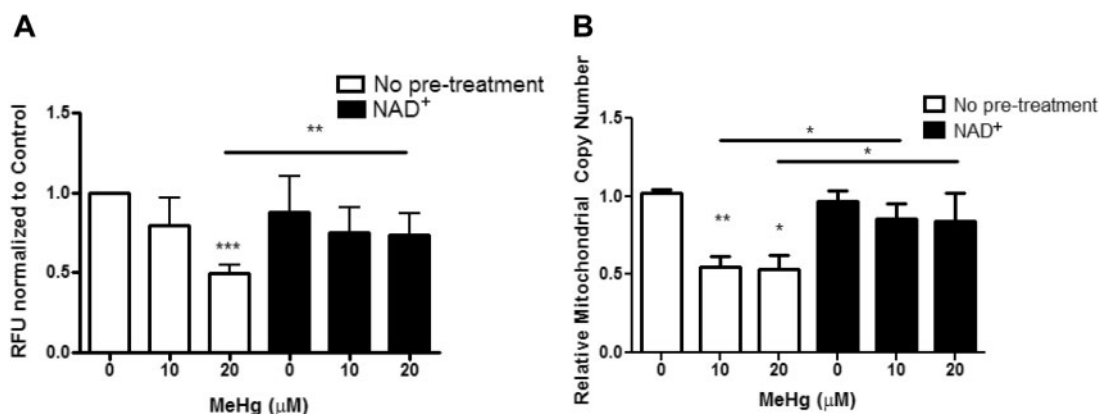
Fig. 5. MeHg decreases mitochondrial mass, which is attenuated by NAD^{+} pretreatmemt. A, OH7193 stained with MitoTracker Green FM and treated with MeHg ± 1 mM NAD^{+} pretreatment to measure mitochondrial mass. Data are a ratio of green to red fluorescence to normalize by worm number from five independent experiments. B, Mitochondrial DNA copy number measured from extracts of N2 worms treated with MeHg ± 1 mM NAD^{+} pretreatment. Data are expressed as means ± SEM from seven independent experiments. *$P < .05$, **$P < .01$,***$P < .001$ as compared with untreated control.

Next, we assessed whether MeHg affected mitochondrial DNA copy number. Both inorganic (Hg) and MeHg have been shown to be genotoxic (Crespo-Lopez *et al.*, 2007; Grotto *et al.*, 2009; Pieper *et al.*, 2014), however the effect of MeHg on the mitochondrial genome has not been investigated. Mitochondrial copy number was measured in worms treated with 10 or 20 μM MeHg in the presence or absence of 1 mM NAD^{+} pretreatment. MeHg significantly decreased the mitochondrial DNA copy number (Figure 5B). NAD^{+} supplementation increased the mitochondrial DNA copy number in response to MeHg to levels similar to untreated control (Figure 5B).

As MeHg decreased mitochondrial mass and replicative capacity of mitochondria, we next investigated whether there was a decrease in oxygen consumption and mitochondrial function. OCR was measured in worms treated with 20 μM MeHg in the presence or absence of 1 mM NAD^{+} pretreatment. Surprisingly, there was no change in OCR following MeHg treatment or in worms treated with NAD^{+} (Supplementary Figure 1). Likewise, other mitochondrial function measures obtained from the Seahorse Bioanalyzer, such as extracellular acidification rate, showed no change across treatments as well (data not shown).

As there appears to be less mitochondria and lower ability of mitochondria to replicate following MeHg treatment, but similar OCR, we hypothesized that there may be damage to the ETC that would cause electrons to leak. It has been observed that MeHg damages complexes II, III, and IV (Mori *et al.*, 2007, 2011; Qu *et al.*, 2013), which can allow for the formation of ROS by combining electrons with oxygen in the inner membrane space rather than in the mitochondrial matrix in the formation of H_2O and ATP by complex V. To determine whether there was increased mitochondrial-derived ROS and damage to the mitochondrial membrane potential, N2 worms were loaded with MitoTracker Red CM-H_2XROS. Worms were then treated with 10 or 20 μM MeHg in the presence or absence of 1 mM NAD^{+} pretreatment. At both doses, MeHg increased the level of mitochondrial-derived ROS, causing a significant increase in red fluorescence (Figure 6). This correlates to a loss in mitochondrial membrane potential (Buckman *et al.*, 2001; Isenberg and Klaunig, 2000). NAD^{+} supplementation prevented the increase in mitochondrial-derived ROS and loss of membrane potential, showing red fluorescence similar to untreated control worms (Figure 6).

NAD^{+} Supplementation Improves Measures of Oxidative Stress in Response to MeHg

Oxidative stress is a hallmark of MeHg exposure. We therefore, investigated whether NAD^{+} supplementation could prevent oxidative stress derived from MeHg treatment in *C. elegans*. ROS damage cellular biomacromolecules, such as proteins and lipids. Proteins can be directly oxidized by ROS, or oxidized lipids can adduct on to the amino acids cysteine, lysine, and histidine through Michael addition chemistry forming carbonyl groups. Levels of oxidized proteins were measured to assess oxidative damage from ROS upon MeHg exposure. A colorimetric assay using DNPH was used to quantify carbonyl adducts on proteins in samples derived from lysates of N2 worms treated with 20 μM MeHg in the presence or absence of 1 mM NAD^{+} pretreatment. MeHg significantly increased protein carbonyl content, which was prevented by NAD^{+} treatment (Figure 7A).

We next investigated the worms' ability to mount an antioxidant response to MeHg upon NAD^{+} supplementation. GSH is the main intracellular thiol that is responsible for maintaining the redox environment of the cell. Upon entering cells, MeHg binds free thiols, such as GSH. Treatment with 10 or 20 μM MeHg led to a 20% decrease in total GSH levels (Figure 7B). Pretreatment with NAD^{+}, prevented the loss in GSH levels by MeHg (Figure 7B). To determine whether the increase in GSH levels in NAD^{+}- and MeHg-treated worms was due either to less oxidative stress or increased formation of GSH, we measured activity of the antioxidant response element (ARE) using the reporter strain VP596. GSH is formed from a two-step process, where the rate-limiting enzyme is controlled by Nrf2 (SKN-1 in *C. elegans*) transcription. We have previously shown that MeHg induces nrf2/SKN-1 in cell culture *C. elegans* (Martinez-Finley *et al.*, 2013; Ni *et al.*, 2010). VP596 expresses GFP under the control of the promoter for the SKN-1 target *gst*-4. MeHg treatment significantly increases the amount of GFP fluorescence (Figure 7C), indicating increased SKN-1 activity. Pretreatment with NAD^{+} decreases the amount of GFP fluorescence produced with MeHg treatment (Figure 7C). This suggests that there is less SKN-1 activity in the NAD^{+} treated worms.

DISCUSSION

MeHg is a known neurotoxin that leads to oxidative stress, cellular dysfunction, and neuronal death. We have previously
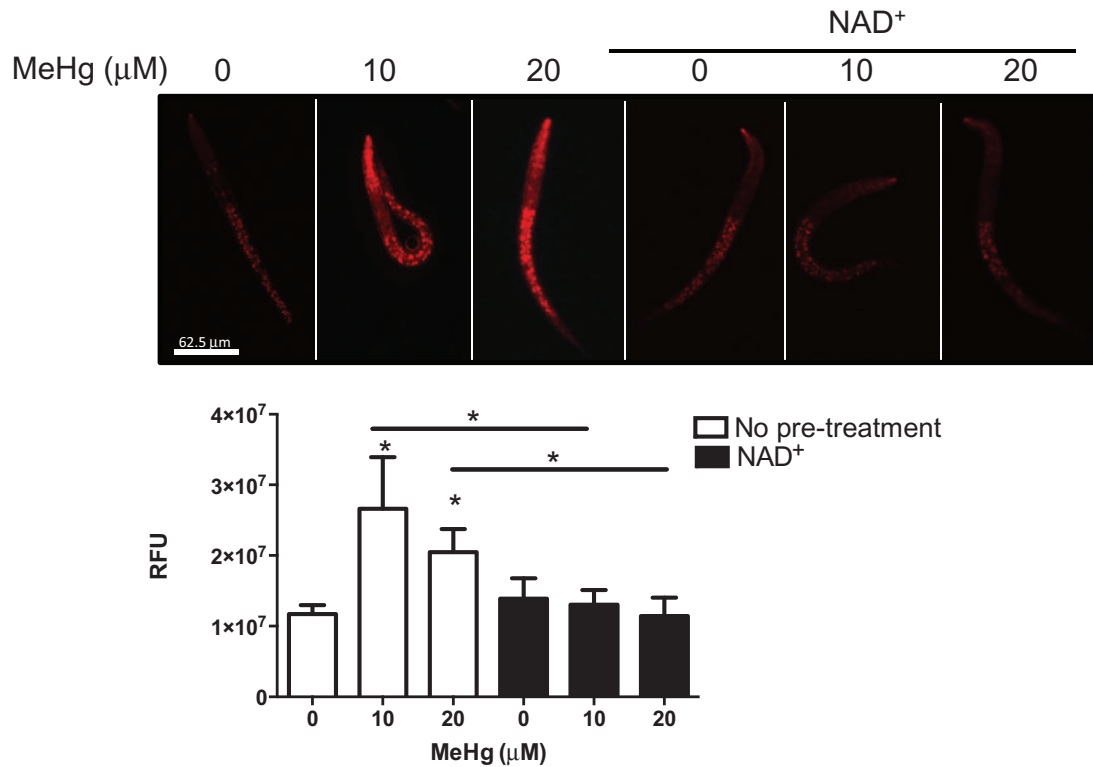
Fig. 6. NAD$^+$ pretreatement improves mitochondrial membrane potential and decreases mitochondrial reactive oxygen species in response to MeHg. Confocal images of N2 worms stained with MitoTracker Red CM-H$_2$XROS and treated with MeHg $\pm$ 1 mM NAD$^+$ pretreatment, with quantification of the red fluorescence. Data are expressed as means $\pm$ SEM from four independent experiments. *$P < .05$ as compared with untreated control.
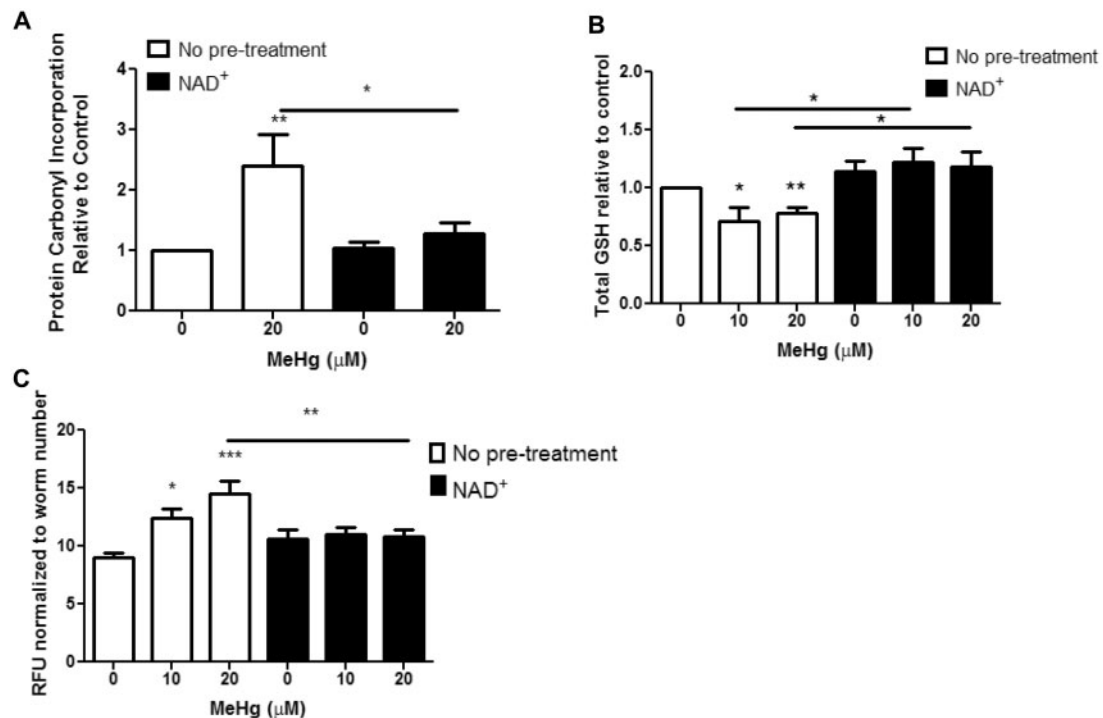

Fig. 7. NAD$^+$ pretreatment decreases MeHg-induced oxidative stress. A, Protein oxidation was measured after 30-min treatment with MeHg $\pm$ 1 mM NAD$^+$ pretreatment. Data are expressed as means $\pm$ SEM from six independent experiments. B, Total GSH levels were measured after 30-min treatment with MeHg $\pm$ 1 mM NAD$^+$ pretreatment. Data are expressed as means $\pm$ SEM from four independent experiments. C, Quantification of GFP fluorescence of VP596 transgenic worms expressing GFP under the gst-4 promoter treated with MeHg $\pm$ 1 mM NAD$^+$ pretreatment. Data are expressed as means $\pm$ SEM from 13 independent experiments. *$P < .05$, **$P < .01$, ***$P < .001$ as compared with untreated control. Abbreviation: GFP, green fluorescent protein; GSH, glutathione.

shown that an early exposure of MeHg in *C. elegans* leads to later life-stage DAergic dysfunction and neurodegeneration (Martinez-Finley *et al.*, 2013). Additionally, DAergic dysfunction in MeHg exposure is dependent on the oxidative stress response, as knockdown of the antioxidant transcription factor *skn-1* sensitizes the worms to MeHg DAergic neurotoxicity (Martinez-Finley *et al.*, 2013; Vanduyn *et al.*, 2010). Due to the high affinity of MeHg for thiol and selenol groups, the redox environment of cells is severely altered by the presence of MeHg. This has multiple consequences from DNA and protein oxidation, mitochondrial dysfunction, and activation of *skn-1*/Nrf2 by MeHg-GSH adducts (Branco *et al.*, 2014; Yoshida *et al.*, 2014). NAD^+ is an important coenzyme that redox cycles and is involved in many processes altered by MeHg. Our data are the first to describe how NAD^+ levels are an important determinant of MeHg toxicity and neurodegeneration.

NAD^+ levels are controlled by both *de novo* synthesis from dietary precursors and from recycling of nicotinamide into the NAD^+ pool through the action of the NAD^+ salvage pathway (Massudi *et al.*, 2012). Maintenance of a NAD^+ pool is important for mitochondrial function (being involved in the citric acid cycle), DNA damage repair (as a substrate for PARPs), protein posttranslational modification (as a substrate for sirtuins), cell signaling (as a substrate for CD38), and for antioxidant enzyme function (as substrate for NAD kinase to produce NADPH) (Chini, 2009; Imai and Guarente, 2014; Morales *et al.*, 2014). Activation of these pathways has been observed with NAD^+ supplementation in a variety of cells *in vitro* and in rodents *in vivo* (Batra and Kislay, 2013; Cerutti *et al.*, 2014; Imai and Guarente, 2014). MeHg exposure depletes cellular NAD^+ levels in *C. elegans* similarly as was observed in heart tissue (Hamdy and Noyes, 1977). Supplementation of worms with excess NAD^+ prevents loss of cellular NAD^+ and provides protection from MeHg lethality. Conversely genetic depletion of NAD^+, through mutation in the NAD^+ salvage pathway, sensitizes worms to MeHg toxicity (Figure 2). Although there have been no reports on decreased viability of the *pnc-1* mutant worms, disruption of NAD^+-dependent processes in this mutant strain leads to a variety of developmental problems, including abnormal muscle differentiation and reproductive impairment (Vrablik *et al.*, 2009, 2011; Wang *et al.*, 2015). Our data suggest a role for maintenance of NAD^+ levels for susceptibility to MeHg.

We have previously demonstrated that MeHg induces a progressive loss of DAergic cell deficits through the use of fluorescent *C. elegans* strains (Martinez-Finley *et al.*, 2013). In our current work, we have found that NAD^+ supplementation can prevent both morphological alterations associated with MeHg exposure and the behavioral deficits. Similarly, NAD^+ supplementation also prevents neurodegeneration associated with manganese-induced hearing loss (Wang *et al.*, 2014). Although the direct effect of NAD^+ levels on DAergic neurons in PD models has not previously been reported, there are mixed reports on protective effects of NAD^+-dependent enzymes. Activation of SIRT1, SIRT3, or SIRT5 provides protection against MPTP, whereas SIRT2 enhances MPTP toxicity in mouse brain (Liu *et al.*, 2014, 2015a,b; Park *et al.*, 2011). We observed that in the *pnc-1* mutant strain, there is constitutive DAergic behavioral deficit, which can be exacerbated by MeHg. Supplementation of NAD^+ may improve DA cell function, as it has been observed that formation of DA quinones can alter the NAD^+/NADH levels, which may lead to mitochondrial dysfunction in PD (Bisaglia *et al.*, 2010). Indeed, loss in DA cell morphology and DAergic behavior from MeHg exposure has been linked to oxidative stress, as worms that express mutant *skn-1*, show exacerbated damage

to the DA system following MeHg exposure (Martinez-Finley *et al.*, 2013; Vanduyn *et al.*, 2010).

Mitochondrial dysfunction is one proposed mechanisms for DAergic degeneration associated in PD (Blesa *et al.*, 2015; Haddad and Nakamura, 2015). Several of genes associated with familial PD are involved in mitochondrial processes such as mitophagy (parkin and PINK1) and metal dyshomeostasis also effects mitochondrial function (Haddad and Nakamura, 2015; Roth, 2014). Our data show that MeHg decreases total numbers of mitochondria and the mitochondria present have diminished replicative capacity due to decreased DNA copy numbers. NAD^+ supplementation prevented the loss of mitochondrial mass and mitochondrial DNA copy numbers in response to MeHg. Similarly, NAD-boosting drugs have been shown to improve mitochondrial function in a fibroblast model of mitochondrial diseases associated with defective complex I function (Felici *et al.*, 2015). In our study, there was no change in oxygen consumption in the worms with either MeHg or NAD^+ treatments. This is in agreement with Cambier *et al.* (2012), which showed no changes in brain mitochondrial respiration in zebrafish exposed to MeHg. However, in rats exposed to a subacute dose of MeHg (10 mg/kg for 5 days), there is elevated mitochondrial oxygen consumption in the cerebellum and cerebrum (Mori *et al.*, 2007). These differences may be due to species differential responses to MeHg or to the diverse cell populations of the examined tissues.

Mitochondrial damage by MeHg has been shown to increase ROS and lead to cellular damage. In rats, MeHg inhibits the ETC, thereby increasing mitochondrial-derived superoxide production and disrupting the mitochondrial membrane potential (Mori *et al.*, 2011; Qu *et al.*, 2013). We found that this similarly occurs in worms, and that NAD^+ supplementation is protective. Our data examining the effects of NAD^+ on MeHg-induced oxidative stress corroborate previous observations, showing suppressed mitochondrial derived ROS (Mori *et al.*, 2007, 2011; Qu *et al.*, 2013). ROS derived from mitochondria upon exposure to MeHg can illicit damage to cellular components. In our system, MeHg increased protein oxidation, decreased cellular GSH levels, and activated ARE-dependent transcription. NAD+ treatment prevented the protein oxidation and there was subsequently less activation of ARE-dependent transcription.

Both mitochondrial dysfunction and oxidative stress have been implicated in the pathogenesis of DAergic neurodegeneration associated with PD (Blesa *et al.*, 2015; Haddad and Nakamura, 2015; Roth, 2014). Our data measuring mitochondrial dysfunction and oxidative stress markers were performed on the whole worm, showing that the effects of MeHg on these parameters are global, whereas the degeneration of the DAergic neurons and loss of DAergic behavior by MeHg is a cell-specific phenomena. These observations are similar to what is seen in humans; markers of inflammation and oxidative stress have been found in plasma of patients with PD (Andican *et al.*, 2012), suggesting that there are systemic alterations in PD. DAergic neurons are hypothesized to be more sensitive to stressors than other cell types, possibly due to their containing DA, which can autoxidize and form dangerous quinones (Hattoria *et al.*, 2009). Therefore, global phenomena, such as MeHg exposure, which may not lead to neurodegeneration or gross morphological changes in most cell types, may affect DAergic neurons more severely.

Altogether, this study demonstrates a significant role for NAD^+ in MeHg toxicity. MeHg decreases cellular NAD^+ levels, which can have detrimental effects on DAergic cell function. Supplementation of NAD^+ provides protection from

MeHg-induced DAergic neurodegeneration, oxidative stress, and mitochondrial dysfunction. Further investigation into the therapeutic potential of NAD$^+$ for MeHg toxicity is warranted, as NAD$^+$is a small, naturally occurring dietary compound that is readily available and shows no toxicity of its own.

ACKNOWLEDGMENTS

Funding

SUPPLEMENTARY DATA

Supplementary data are available online at http://toxsci. oxfordjournals.org/.

REFERENCES

Andican, G., Konukoglu, D., Bozluolcay, M., Bayulkem, K., Firtiina, S., and Burcak, G. (2012). Plasma oxidative and inflammatory markers in patients with idiopathic Parkinson's disease. *Acta Neurol. Belg.* **112**, 155–159.

Araki, T., Sasaki, Y., and Milbrandt, J. (2004). Increased nuclear NAD biosynthesis and SIRT1 activation prevent axonal degeneration. *Science* **305**, 1010–1013. '

Batra, V., and Kislay, B. (2013). Mitigation of gamma-radiation induced abasic sites in genomic DNA by dietary nicotinamide supplementation: Metabolic up-regulation of NAD(+) biosynthesis. *Mutat. Res.* **749**, 28–38.

Bisaglia, M., Soriano, M. E., Arduini, I., Mammi, S., and Bubacco, L. (2010). Molecular characterization of dopamine-derived quinones reactivity toward NADH and glutathione: implications for mitochondrial dysfunction in Parkinson disease. *Biochim. Biophys. Acta* **1802**, 699–706.

Blesa, J., Trigo-Damas, I., Quiroga-Varela, A., and Jackson-Lewis, V. R. (2015). Oxidative stress and Parkinson's disease. *Front. Neuroanat.* **9**, 91.

Bornhorst, J., Chakraborty, S., Meyer, S., Lohren, H., Brinkhaus, S. G., Knight, A. L., Caldwell, K. A., Caldwell, G. A., Karst, U., Schwerdtle, T., *et al.* (2014). The effects of pdr1, djr1.1 and pink1 loss in manganese-induced toxicity and the role of alpha-synuclein in C. *elegans*. *Metallomics* **6**, 476–490.

Branco, V., Godinho-Santos, A., Goncalves, J., Lu, J., Holmgren, A., and Carvalho, C. (2014). Mitochondrial thioredoxin reductase inhibition, selenium status, and Nrf-2 activation are determinant factors modulating the toxicity of mercury compounds. *Free Radic. Biol. Med.* **73**, 95–105.

Brenner, S. (1974). The genetics of Caenorhabditis elegans. *Genetics* **77**, 71–94.

Buckman, J. F., Hernandez, H., Kress, G. J., Votyakova, T. V., Pal, S., and Reynolds, I. J. (2001). MitoTracker labeling in primary neuronal and astrocytic cultures: Influence of mitochondrial membrane potential and oxidants. *J. Neurosci. Methods* **104**, 165–176.

Caito, S. W., and Aschner, M. (2015). Quantification of glutathione in Caenorhabditis elegans. *Curr. Protoc. Toxicol.* **64**, 6.18.1–6.18.6.

Cambier, S., Gonzalez, P., Mesmer-Dudons, N., Brethes, D., Fujimura, M., and Bourdineaud, J. P. (2012). Effects of dietary methylmercury on the zebrafish brain: Histological, mitochondrial, and gene transcription analyses. *Biometals* **25**, 165–180.

Carvalho, C. M., Chew, E. H., Hashemy, S. I., Lu, J., and Holmgren, A. (2008). Inhibition of the human thioredoxin system. A molecular mechanism of mercury toxicity. *J. Biol. Chem.* **283**, 11913–11923.

Cerutti, R., Pirinen, E., Lamperti, C., Marchet, S., Sauve, A. A., Li, W., Leoni, V., Schon, E. A., Dantzer, F., Auwerx, J., *et al.* (2014). NAD(+)- dependent activation of Sirt1 corrects the phenotype in a mouse model of mitochondrial disease. *Cell Metab.* **19**, 1042–1049.

Chini, E. N. (2009). CD38 as a regulator of cellular NAD: A novel potential pharmacological target for metabolic conditions. *Curr. Pharm. Des.* **15**, 57–63.

Clarkson, T. W., and Magos, L. (2006). The toxicology of mercury and its chemical compounds. *Crit. Rev. Toxicol.* **36**, 609–662.

Crespo-Lopez, M. E., Lima de Sa, A., Herculano, A. M., Rodriguez, R B., and Martins do Nascimento, J. L., (2007). Methylmercury genotoxicity: A novel effect in human cell lines of the central nervous system. *Environ. Int.* **33**, 141–146.

Ding, D., Qi, W., Yu, D., Jiang, H., Han, C., Kim, M. J., Katsuno, K., Hsieh, Y. H., Miyakawa, T., Salvi, R., *et al.* (2013). Addition of exogenous NAD+ prevents mefloquine-induced neuroaxonal and hair cell degeneration through reduction of caspase-3-mediated apoptosis in cochlear organotypic cultures. *PLoS One* **8**, e79817

Ekino, S., Susa, M., Ninomiya, T., Imamura, K., and Kitamura, T. (2007). Minamata disease revisited: an update on the acute and chronic manifestations of methyl mercury poisoning. *J. Neurol. Sci.* **262**, 131–144.

Farina, M., Aschner, M., and Rocha, J. B. (2011). Oxidative stress in MeHg-induced neurotoxicity. *Toxicol. Appl. Pharmacol.* **256**, 405–417.

Farina, M., Campos, F., Vendrell, I., Berenguer, J., Barzi, M., Pons, S., and Sunol, C. (2009). Probucol increases glutathione peroxidase-1 activity and displays long-lasting protection against methylmercury toxicity in cerebellar granule cells'. *Toxicol. Sci.* **112**, 416–426.

Felici, R., Lapucci, A., Cavone, L., Pratesi, S., Berlinguer-Palmini, R., and Chiarugi, A. (2015). Pharmacological NAD-boosting strategies improve mitochondrial homeostasis in human complex I-mutant fibroblasts. *Mol. Pharmacol.* **87**, 965–971.

Gavet, O., and Pines, J. (2010). Progressive activation of CyclinB1-Cdk1 coordinates entry to mitosis. *Dev. Cell* **18**, 533–543.

Grandjean, P., Satoh, H., Murata, K., and Eto, K. (2010). Adverse effects of methylmercury: environmental health research implications. *Environ. Health Perspect.* **118**, 1137–1145.

Grotto, D., Barcelos, G. R., Valentini, J., Antunes, L. M., Angeli, J. P., Garcia, S. C., and Barbosa, F. Jr. (2009). Low levels of methylmercury induce DNA damage in rats: Protective effects of selenium. *Arch. Toxicol.* **83**, 249–254.

Haddad, D., and Nakamura, K. (2015). Understanding the susceptibility of dopamine neurons to mitochondrial stressors in Parkinson's disease. *FEBS Lett.* **589**, 3702–3713

Hamdy, M. K., and Noyes, O. R. (1977). Effect of mercury on NADH and the protective role of oxalacetate. *Bull. Environ. Contam. Toxicol.* **17**, 112–120.

Hattoria, N., Wanga, M., Taka, H., Fujimura, T., Yoritaka, A., Kubo, S., and Mochizuki, H. (2009). Toxic effects of dopamine metabolism in Parkinson's disease. *Parkinsonism Relat. Disord.* 15(Suppl 1), S35–S38.

Herculano, A. M., Crespo-Lopez, M. E., Lima, S. M., Picanco-Diniz, D. L., and Do Nascimento, J. L. (2006). Methylmercury intoxication activates nitric oxide synthase in chick retinal cell culture. *Braz. J. Med. Biol. Res.* **39**, 415–418.

Imai, S., and Guarente, L. (2014). NAD+ and sirtuins in aging and disease. *Trends Cell Biol* **24**, 464–471.

Isenberg, J. S., and Klaunig, J. E. (2000). Role of the mitochondrial membrane permeability transition (MPT) in rotenone-induced apoptosis in liver cells. *Toxicol Sci.* **53**, 340–351.

Landrigan, P. J., Sonawane, B., Butler, R. N., Trasande, L., Callan, R., and Droller, D. (2005). Early environmental origins of neurodegenerative disease in later life. *Environ. Health Perspect.* **113**, 1230–1233.

Liu, L., Arun, A., Ellis, L., Peritore, C., and Donmez, G. (2014). SIRT2 enhances 1-methyl-4-phenyl-1,2,3,6-tetrahydropyridine (MPTP)-induced nigrostriatal damage via apoptotic pathway. *Front. Aging Neurosci.* **6**, 184.

Liu, L., Peritore, C., Ginsberg, J., Kayhan, M., and Donmez, G. (2015a). SIRT3 attenuates MPTP-induced nigrostriatal degeneration via enhancing mitochondrial antioxidant capacity. *Neurochem. Res.* **40**, 600–608.

Liu, L., Peritore, C., Ginsberg, J., Shih, J., Arun, S., and Donmez, G. (2015b). Protective role of SIRT5 against motor deficit and dopaminergic degeneration in MPTP-induced mice model of Parkinson's disease. *Behav. Brain Res.* **281**, 215–221.

Luz, A. L., Smith, L. L., Rooney, J. P., and Meyer, J. N. 2015. Seahorse Xf(e) 24 extracellular flux analyzer-based analysis of cellular respiration in Caenorhabditis elegans. *Curr. Protoc. Toxicol.* **66**, 25 7 1–25 7 15.

Martinez-Finley, E. J., Caito, S., Slaughter, J. C., and Aschner, M. (2013). The role of skn-1 in methylmercury-induced latent dopaminergic neurodegeneration. *Neurochem. Res.* **38**, 2650–2660.

Massudi, H., Grant, R., Guillemin, G. J., and Braidy, N. (2012). NAD+ metabolism and oxidative stress: The golden nucleotide on a crown of thorns. *Redox Rep.* **17**, 28–46.

Morales, J., Li, L., Fattah, F. J., Dong, Y., Bey, E. A., Patel, M., Gao, J., and Boothman, D. A. (2014). Review of poly (ADP-ribose) polymerase (PARP) mechanisms of action and rationale for targeting in cancer and other diseases. *Crit. Rev. Eukaryot. Gene Expr.* **24**, 15–28.

Mori, N., Yasutake, A., and Hirayama, K. (2007). Comparative study of activities in reactive oxygen species production/defense system in mitochondria of rat brain and liver, and their susceptibility to methylmercury toxicity. *Arch. Toxicol.* **81**, 769–776.

Mori, N., Yasutake, A., Marumoto, M., and Hirayama, K. (2011). Methylmercury inhibits electron transport chain activity and induces cytochrome c release in cerebellum mitochondria'. *J. Toxicol. Sci.* **36**, 253–259.

Ni, M., Li, X., Yin, Z., Jiang, H., Sidoryk-Wegrzynowicz, M., Milatovic, D., Cai, J., and Aschner, M. (2010). Methylmercury induces acute oxidative stress, altering Nrf2 protein level in primary microglial cells. *Toxicol. Sci.* **116**, 590–603.

Park, G., Jeong, J. W., and Kim, J. E. (2011). SIRT1 deficiency attenuates MPP+-induced apoptosis in dopaminergic cells. *FEBS Lett.* **585**, 219–224.

Petersen, M. S., Halling, J., Bech, S., Wermuth, L., Weihe, P., Nielsen, F., Jorgensen, P. J., Budtz-Jorgensen, E., and Grandjean, P. (2008). Impact of dietary exposure to food contaminants on the risk of Parkinson's disease. *Neurotoxicology* **29**, 584–590.

Pieper, I., Wehe, C. A., Bornhorst, J., Ebert, F., Leffers, L., Holtkamp, M., Hoseler, P., Weber, T., Mangerich, A., Burkle, A., *et al.* (2014). Mechanisms of Hg species induced toxicity in cultured human astrocytes: Genotoxicity and DNA-damage response. *Metallomics* **6**, 662–671.

Qu, M., Nan, X., Gao, Z., Guo, B., Liu, B., and Chen, Z. (2013). Protective effects of lycopene against methylmercury-induced neurotoxicity in cultured rat cerebellar granule neurons. *Brain Res.* **1540**, 92–102.

Rooney, J. P., Ryde, I. T., Sanders, L. H., Howlett, E. H., Colton, M. D., Germ, K. E., Mayer, G. D., Greenamyre, J. T., and Meyer, J. N. (2015). PCR based determination of mitochondrial DNA copy number in multiple species. *Methods Mol. Biol.* **1241**, 23–38.

Roth, J. A. (2014). Correlation between the biochemical pathways altered by mutated Parkinson-related genes and chronic exposure to manganese. *Neurotoxicology* **44**, 314–325.

Sawin, E. R., Ranganathan, R., and Horvitz, H. R. (2000). C. elegans locomotory rate is modulated by the environment through a dopaminergic pathway and by experience through a serotonergic pathway. *Neuron* **26**, 619–631.

Shanker, G., Aschner, J. L., Syversen, T., and Aschner, M. (2004). Free radical formation in cerebral cortical astrocytes in culture induced by methylmercury. *Brain Res. Mol. Brain Res.* **128**, 48–57.

Stiernagle, T. 1999. Maintenance of *C. elegans*. In *C. elegans: A Practical Approach* Hope. (I.A, ed.), Oxford University Press, New York, NY.

Vanduyn, N., Settivari, R., Wong, G., and Nass, R. (2010). SKN-1/Nrf2 inhibits dopamine neuron degeneration in a Caenorhabditis elegans model of methylmercury toxicity. *Toxicol. Sci.* **118**, 613–624.

Vrablik, T. L., Huang, L., Lange, S. E., and Hanna-Rose, W. (2009). Nicotinamidase modulation of NAD+ biosynthesis and nicotinamide levels separately affect reproductive development and cell survival in C. elegans. *Development* **136**, 3637–3646.

Vrablik, T. L., Wang, W., Upadhyay, A., and Hanna-Rose, W. (2011). Muscle type-specific responses to NAD+ salvage biosynthesis promote muscle function in Caenorhabditis elegans. *Dev. Biol.* **349**, 387–394.

Wang, J., Zhai, Q., Chen, Y., Lin, E., Gu, W., McBurney, M. W., and He, Z. (2005). A local mechanism mediates NAD-dependent protection of axon degeneration. *J. Cell Biol.* **170**, 349–355.

Wang, L., Ding, D., Salvi, R., and Roth, J. A. (2014). Nicotinamide adenine dinucleotide prevents neuroaxonal degeneration induced by manganese in cochlear organotypic cultures. *Neurotoxicology* **40**, 65–74.

Wang, W., McReynolds, M. R., Goncalves, J. F., Shu, M., Dhondt, I., Braeckman, B. P., Lange, S. E., Kho, K., Detwiler, A. C., Pacella, M. J., *et al.* (2015). Comparative metabolomic profiling reveals that dysregulated glycolysis stemming from lack of salvage nad+ biosynthesis impairs reproductive development in Caenorhabditis elegans. *J. Biol. Chem.* **290**, 26163–26179.

Weiss, B., Clarkson, T. W., and Simon, W. (2002). Silent latency periods in methylmercury poisoning and in neurodegenerative disease. *Environ. Health Perspect.* **110**(Suppl 5), 851–854.

Yasuda, K., Adachi, H., Fujiwara, Y., and Ishii, N. (1999). Discussion B52-3 protein carbonyl accumulation in aging

dauer formation-defective (daf) mutants of Caenorhabditis elegans. *J. Gerontol. A. Biol. Sci. Med. Sci.* **54**, B47–B51.

Yoshida, E., Abiko, Y., and Kumagai, Y. (2014). Glutathione adduct of methylmercury activates the Keap1-Nrf2 pathway in SH-SY5Y cells. *Chem. Res. Toxicol.* **27**, 1780–1786.

Zhou, M., Ottenberg, G., Sferrazza, G. F., Hubbs, C., Fallahi, M., Rumbaugh, G., Brantley, A. F., and Lasmezas, C. I. (2015). Neuronal death induced by misfolded prion protein is due to NAD+ depletion and can be relieved in vitro and in vivo by NAD+ replenishment. *Brain* **138**, 992–1008.